Atmos. Chem. Phys. Discuss., 13, 27779–27810, 2013
www.atmos-chem-phys-discuss.net/13/27779/2013/
doi:10.5194/acpd-13-27779-2013

Atmospheric Chemistry and Physics
Discussions
Open Access

Emission factor ratios, SOA mass yields, and the impact of vehicular emissions on SOA formation

J. J. Ensberg[1], P. L. Hayes[2,3,*], J. L. Jimenez[2,3], J. B. Gilman[3,4], W. C. Kuster[4], J. A. de Gouw[3,4], J. S. Holloway[3,4], and J. H. Seinfeld[1,5]

[1] Division of Chemistry and Chemical Engineering, California Institute of Technology, Pasadena, California, USA
[2] Department of Chemistry and Biochemistry, University of Colorado, Boulder, Colorado, USA
[3] Cooperative Institute for Research in Environmental Sciences, University of Colorado Boulder, Boulder, Colorado, USA
[4] Chemical Sciences Division, Earth System Research Laboratory, NOAA, Boulder, Colorado, USA
[5] Division of Engineering and Applied Science, California Institute of Technology, Pasadena, California, USA
[*] now at: Department of Chemistry, University of Montreal, Montreal, Quebec, Canada

Received: 17 September 2013 – Accepted: 19 October 2013 – Published: 28 October 2013

Correspondence to: J. H. Seinfeld (seinfeld@caltech.edu)

Published by Copernicus Publications on behalf of the European Geosciences Union.

Abstract

The underprediction of ambient secondary organic aerosol (SOA) levels by atmospheric models in urban areas is well established, yet the cause of this underprediction remains elusive. Likewise, the relative contribution of emissions from gasoline- and diesel-fueled vehicles to the formation of SOA is generally unresolved. Here we address these two issues using data from the 2010 CalNex experiment carried out in the Los Angeles basin (Ryerson et al., 2013). We use gas-phase organic mass (GPOM) and CO emission factors in conjunction with measured enhancements in oxygenated organic aerosol (OOA) relative to CO to investigate the relative importance of gasoline vs. diesel emissions to organic aerosol formation. Two possible conclusions emerge from the analysis to yield consistency with the ambient data: (1) vehicular emissions are not a dominant source of anthropogenic fossil SOA in the Los Angeles basin, or (2) ambient SOA mass yields are substantially higher than those derived from laboratory chamber studies.

1 Introduction

Emissions in California have significantly decreased over time (Warneke et al., 2012). However, two important issues concerning the sources of organic aerosol in urban areas remain generally unresolved: (1) what is the relative impact of emissions from gasoline- and diesel-fueled vehicles on the formation of secondary organic aerosol (SOA) (Bahreini et al., 2012; Gentner et al., 2012; Hayes et al., 2013); (2) what is the cause of the significant underprediction of SOA levels by existing atmospheric models in urban areas (de Gouw et al., 2005; Volkamer et al., 2006; Johnson et al., 2006; de Gouw et al., 2008; Kleinman et al., 2008; Matsui et al., 2009)? We address here these two issues based on a detailed analysis of data in the Los Angeles atmosphere; analysis of these issues is likely to be applicable to major urban areas worldwide. Based on the highly resolved speciation profiles of gasoline and diesel fuel, Gentner et al. (2012)

estimated that diesel exhaust is responsible for 2 to 7 times more SOA than gasoline exhaust in California. On the other hand, from measurements of the weekday-weekend cycle of organic aerosol, black carbon, single-ring aromatic hydrocarbons, CO, and oxides of nitrogen ($NO_x = NO + NO_2$) in the Los Angeles Basin, Bahreini et al. (2012) and Hayes et al. (2013) conclude that emissions from gasoline-fueled vehicles dominate the SOA budget. Notably, the conclusions of Bahreini et al. (2012) and Hayes et al. (2013) are based on the observation that diesel activity has a clear weekday-weekend cycle, whereas measured CO mixing ratios and the enhancement of SOA with respect to CO exhibit virtually no weekday-weekend cycle when segregated by photochemical age. Nevertheless, as acknowledged by Hayes et al. (2013), the conclusions of Bahreini et al. (2012) and Hayes et al. (2013) presume that vehicular emissions are the dominant source of anthropogenic fossil SOA in the L.A. Basin.

2 Ambient measurements

Ambient data (CO, NO_x, NO_y, O_3, OH, VOCs, submicron non-refractory (nrPM1) organic aerosol) at the Pasadena ground site were collected during the 2010 CalNex experiment (Ryerson et al., 2013). The CalNex Pasadena ground site was located 18 km northeast of downtown Los Angeles on the California Institute of Technology (Caltech) campus in Pasadena, California (34.1406° N, 118.1225° W, 236 m above mean sea level). The measurement period was 15 May 2010 00:00–16 June 2010 00:00 (LT). The prevailing wind direction during daytime in Pasadena was from the southwest due to the sea-breeze, which brought air masses from the Pacific Ocean across central Los Angeles to Pasadena.

CO concentrations were measured by two vacuum-UV resonance fluorescence instruments (AL5001 and AL5002, Aerolaser) (Gerbig et al., 1999). A Fluorescence Assay by Gas Expansion (FAGE) instrument was utilized to determine the OH concentration (Dusanter et al., 2009). The concentration of O_3 was measured by UV differential absorption (49c Ozone Analyzer, Thermo Scientific). An in-situ Gas Chromatography Mass Spectrometry (GC-MS) instrument provided the mixing ratios for a variety of VOCs (Gilman et al., 2009). NO_x and NO_y concentrations were measured using chemiluminescence (42i-TL with Mo converter, Thermo Scientific), and NO_2 was measured with Cavity Enhanced Differential Optical Absorption Spectroscopy (CE-DOAS) (Thalman and Volkamer, 2010). Concentrations of submicron non-refractory (nrPM1) organic aerosol particles were measured using an Aerodyne High Resolution Time-of-Flight Aerosol Mass Spectrometer (hereinafter referred to as "AMS") (DeCarlo et al., 2006). The OA mass spectral matrix was deconvolved into components using PMF, a receptor-based factorization model (Paatero et al., 1994). The OA components from the PMF analysis were identified by their mass spectra, diurnal cycles, and elemental composition, as well as by the concentration ratios and correlations of their time series with tracers. These components are: (1) Hydrocarbon-like Organic Aerosol (HOA), (2) Cooking- Influenced Organic Aerosol (CIOA), (3) Local Organic Aerosol (LOA), (4) Semi-Volatile Oxygenated Organic Aerosol (SV-OOA), and (5) Low-Volatility Oxygenated Organic Aerosol (LV-OOA). The HOA component has been previously described as a surrogate for primary combustion OA, and the SV-OOA and LV-OOA components as surrogates for "fresher" and "aged" SOA, respectively. (Zhang et al., 2007; Aiken et al., 2008; Jimenez et al., 2009; Ulbrich et al., 2009). As discussed in Hayes et al. (2013), the LOA component exhibits high frequency fluctuations most likely resulting from local sources in close proximity to the Pasadena ground site. However, since LOA represents only $\sim 5\,\%$ of the total OA budget, this factor is not considered further.

Figure 1 shows measured PMF factor concentrations normalized by CO enhancement (ΔCO is the difference between the ambient CO and the estimated background CO (105 ppb)) as functions of photochemical age (see Hayes et al. (2013) for a detailed description of how this figure was constructed). The photochemical age of the air mass over the Pasadena site was calculated by two methods: (1) from the ratio of 1,2,4-trimethylbenzene to benzene concentrations, as described in Parrish et al. (2007); and (2) by defining the photochemical age as $-\log_{10}(NO_x/NO_y)$ similar to Kleinman et al.

(2008). Both methods give very similar results, and all photochemical ages were calculated using a reference average OH radical concentration of 1.5×10^6 molecules cm^{-3}. For reference, the daily (day and night) OH radical concentrations averaged over the entire campaign at the Pasadena site was 1.3×10^6 molecules cm^{-3}. Owing to the formation of SOA, the OOA factors are enhanced (increased) with respect to ΔCO as the photochemical age of the air mass increases. As shown in Fig. 1b, the enhancement of OOA (SV-OOA + LV-OOA) relative to ΔCO after 0.45 days of photochemical processing is 48 µg OOA sm^{-3} (ppmvCO)$^{-1}$ (48 is the difference between 58, which occurs at 0.45 days, and 10, which occurs at 0 days), whereas the ratio of POA (HOA + CIOA) to ΔCO is relatively constant (i.e. no enhancement) at 9.6 µg (HOA + CIOA) sm^{-3} (ppmvCO)$^{-1}$. Note that the average OOA enhancement corresponds to an average OH-exposure of 58.3×10^9 molec cm^{-3} s (∼ 0.45 days), and that the average POA/ΔCO value is very similar to the value of 9.4 µg POA sm^{-3} (ppmvCO)$^{-1}$ assumed by both Bahreini et al. (2012) and Gentner et al. (2012).

In this study, we are primarily interested in the fraction of OOA attributable to anthropogenic fossil activity. Based on the ^{14}C analysis presented in Zotter et al. (2013), 70 % of the SV-OOA enhancement represents a conservative lower limit for the fraction of OOA that is attributable to anthropogenic fossil-fuel activity. We note that some anthropogenic SOA such as from cooking emissions will be non-fossil. Therefore, we note that at 0.45 days of photochemical processing, 70 % of the SV-OOA enhancement is equal to $\sim 25 \pm 9$ µg SV – OOA sm^{-3} (ppmvCO)$^{-1}$ (Fig. 1c), where ±9 µg SV – OOA sm^{-3} (ppmvCO)$^{-1}$ is the propagated uncertainty associated with the OOA and CO measurements.

3 Results and discussion

3.1 Emission ratios and required SOA yields

Fuel-sales data reported by the California Department of Transportation (http://www.dot.ca.gov/hq/tsip/otfa/tab/documents/mvstaff/mvstaff08.pdf) indicate that diesel and gasoline fuel sales in California counties upwind of Pasadena during 2010 represented approximately 13 and 87 % of total fuel sales (county-wide) by volume, respectively. Therefore, on average, for every liter of fuel combusted on-road and upwind of Pasadena in 2010, the following can be assumed:

$$[L_{\text{gas}}] = 0.87 \times [L_{\text{fuel}}] \qquad (1)$$

$$[L_{\text{dies}}] = 0.13 \times [L_{\text{fuel}}] \qquad (2)$$

Figure 2a shows the chemical speciation profile and the compound-specific SOA mass yields ($Y = \Delta\text{SOA}/\Delta\text{Hydrocarbon}$) for a composite fuel comprising 13 % diesel fuel and 87 % gasoline fuel (by volume), based on detailed chemical-speciation profiles (see Tables S5, S6 and S8 of Gentner et al., 2012). As shown in Fig. 2a, the 2010 composite fuel composition is dominated by species with fewer than 12 carbon atoms, with the largest contributions coming from branched alkanes and single-ring aromatics. Note that the percentages listed in the legend of Fig. 2a sum to ~ 90 % which corresponds to the unprecedented level of mass closure Gentner et al. (2012) obtained in characterizing gasoline and diesel fuel. Gentner et al. (2012) estimated the SOA mass yields ($Y = \Delta\text{SOA}/\Delta\text{Hydrocarbon}$) for pure gasoline and pure diesel fuel using a combination of measured SOA mass yields derived from laboratory-chamber experiments and approximate SOA mass yields based on box-modeling. The compound-specific SOA mass yields reported by Gentner et al. (2012) are given in Fig. 2b and c shows the product of the estimated yields and the weight percent (by carbon) of the individual species in liquid fuel. In contrast to the cumulative distribution shown in Fig. 2a, roughly 50 % of the expected SOA mass is attributable to species with fewer than 12 carbons and 50 % is attributable to species with more than 12 carbons. Note that single-ring aromatics are predicted to make the most significant contribution to the SOA budget (Fig. 2c).

Vehicular exhaust emissions include water, CO, CO_2, NO_x, and partially combusted hydrocarbons, as well as a large contribution from unburned fuel that escapes combustion. Gentner et al. (2012) argue that unburned fuel in exhaust emissions is the dominant source of newly formed SOA attributable to vehicular activity. Emission factors reported by Gentner et al. (2012), which are based on CalNex 2010 measurements at the Caldecott Tunnel in Oakland, CA, for CO and for noncombusted gas-phase organic mass (GPOM) emitted in the exhaust of gasoline and diesel engines are:

$$\mathrm{EF_{CO,gas}} = 14.7 \pm 5.88\,\mathrm{g\,CO}\ (L_\mathrm{gas})^{-1} \tag{3}$$

$$\mathrm{EF_{CO,dies}} = 4.5 \pm 1.80\,\mathrm{g\,CO}\ (L_\mathrm{dies})^{-1} \tag{4}$$

$$\mathrm{EF_{GPOM,gas}} = 0.45 \pm 0.18\,\mathrm{g\,GPOM}\ (L_\mathrm{gas})^{-1} \tag{5}$$

$$\mathrm{EF_{GPOM,dies}} = 1.01 \pm 0.40\,\mathrm{g\,GPOM}\ (L_\mathrm{dies})^{-1} \tag{6}$$

where the uncertainties are assumed to be ±40 % based on average values reported in Tables S5 and S6 of McDonald et al. (2013). Therefore, the total amount of noncombusted GPOM and CO emitted per liter of combusted fuel is:

$$\mathrm{GPOM} = \mathrm{EF_{GPOM,gas}} \times [L_\mathrm{gas}] + \mathrm{EF_{GPOM,dies}} \times [L_\mathrm{dies}] \tag{7}$$

$$\mathrm{CO} = \mathrm{EF_{CO,gas}} \times [L_\mathrm{gas}] + \mathrm{EF_{CO,dies}} \times [L_\mathrm{dies}] \tag{8}$$

Substituting Eqs. (1) and (2) into Eqs. (7) and (8) and dividing gives the amount of GPOM that is emitted per unit of CO mass emitted (defined here as $\mathrm{EF_{GPOM,CO}}$):

$$\mathrm{EF_{GPOM,CO}} = \frac{[\mathrm{GPOM}]}{[\mathrm{CO}]} = \frac{\mathrm{EF_{GPOM,gas}} \times 0.87 + \mathrm{EF_{GPOM,diesel}} \times 0.13}{\mathrm{EF_{CO,gas}} \times 0.87 + \mathrm{EF_{CO,diesel}} \times 0.13} \tag{9}$$

$$\mathrm{EF_{GPOM,CO}} = 0.039 \pm 0.019\,\mathrm{g\,GPOM\,(g\ CO)^{-1}} \tag{10}$$

Converting g to µg and normalizing the numerator and denominator by air volume at standard conditions (273 K and 1 atm), Eq. (10) can be written as:

$$\mathrm{EF_{GPOM,CO}} = 0.039 \pm 0.019\,\mu\mathrm{g\,GPOM\,sm^{-3}}\,(\mu\mathrm{g\,CO\,sm^{-3}})^{-1} \tag{11}$$

The CO emission units µg CO $\mathrm{sm^{-3}}$ in Eq. (11) can be converted to ppmv CO by using the following conversion factor, which is applicable at 273 K and 1 atm:

$$\begin{aligned}\mathrm{EF_{GPOM,CO}} &= 0.039 \pm 0.019\,\mu\mathrm{g\,GPOM\,sm^{-3}}\,(\mu\mathrm{g\,CO\,sm^{-3}})^{-1} \\ &\quad \times 1250\,\mu\mathrm{g\,CO\,sm^{-3}}\,(\mathrm{ppmv\,CO})^{-1}\end{aligned} \tag{12}$$

$$\mathrm{EF_{GPOM,CO}} = 48.9 \pm 24.3\,\mu\mathrm{g\,CO\,sm^{-3}}\,(\mathrm{ppmv\,CO})^{-1} \tag{13}$$

We assume that $\mathrm{EF_{GPOM,CO}}$ given by Eq. (13) is representative of the average vehicle-fleet, and that the 70 % of the SV-OOA concentrations that are comprised of fossil carbon at the Pasadena ground site are attributable to vehicular emissions (Bahreini et al., 2012; Hayes et al., 2013). Using $\mathrm{EF_{GPOM,CO}}$ and 70 % of the SV-OOA enhancement ($25 \pm 9\,\mu\mathrm{g\,OOA\,sm^{-3}}\,(\mathrm{ppmvCO})^{-1}$) given in Fig. 1b, the average aggregate SOA mass yield required to obtain mass closure at the Pasadena ground site, Y_{req}, can be determined as follows:

$$Y_{\mathrm{req}} = \frac{\Delta\mathrm{SOA}}{\Delta\mathrm{GPOM}} = \frac{25 \pm 9\,\mu\mathrm{g\,SOA\,sm^{-3}}\,(\mathrm{ppmv\,CO})^{-1}}{48.9 \pm 24.3\,\mu\mathrm{g\,GPOM\,sm^{-3}}\,(\mathrm{ppmv\,CO})^{-1}} = 51.1 \pm 31.4\,\% \tag{14}$$

This required overall SOA mass yield is to be compared with the estimated yields reported in Gentner et al. (2012) (Fig. 2) for pure gasoline fuel and pure diesel fuel, which are 2.3 ± 0.7 % and 15 ± 5 %, respectively. For reference, the predicted SOA mass yield for a fuel comprising 87 % gasoline and 13 % diesel is 5.5 % (Fig. 3a). Note that the required SOA mass yield is a lower bound because it is based on the assumption that 100 % of the GPOM reacts within 0.45 days (OH-exposure =∼ 58.3×10^9 molec $\mathrm{cm^{-3}\,s}$) of being emitted. As shown in Table 1, the fraction of hydrocarbon reacted for an

OH-exposure of 58.3×10^9 molec cm^{-3} s is between 0.07 and 0.74 for several hydrocarbons abundant in gasoline and diesel fuel. To account for partial reaction of the emitted hydrocarbons, we reduce each chemical constituent of the emitted GPOM (Fig. 2a) by the fraction that would react after 0.45 days of photochemical aging. The partially reacted $\mathrm{EF_{GPOM,CO}}$ (Eq. 13) is then determined by summing over all partially-reacted GPOM components. The total fraction of GPOM reacted after 0.45 days of photochemical aging ranges from 0.66 at 100 % diesel to 0.43 at 100 % gasoline, and is 0.47 for fuel usage of 13 % diesel and 87 % gasoline (by volume). Reducing the $\mathrm{EF_{GPOM,CO}}$ by a factor of 0.47 increases the required yield by a factor of 2.13 ($Y_\mathrm{req} = 2.13 \times 51.1 \pm 31.4 = 108.7 \pm 66.9$).

The analysis thus far is based on the county-specific fuel usage of 13 % diesel and 87 % gasoline (by volume). However, the dependence of the required overall SOA mass yield on any fractional fuel usage ($f_\mathrm{gas} + f_\mathrm{dies} = 1$) is calculated as:

$$\mathrm{EF_{GPOM,CO}}(f_\mathrm{gas}, f_\mathrm{dies}) = \frac{\mathrm{EF_{GPOM,gas}} \times f_\mathrm{gas} + \mathrm{EF_{GPOM,dies}} \times f_\mathrm{dies}}{\mathrm{EF_{CO,gas}} \times f_\mathrm{gas} + \mathrm{EF_{CO,dies}} \times f_\mathrm{dies}} \times \mathrm{FR}(f_\mathrm{gas}, f_\mathrm{dies}) \tag{15}$$

$$Y_\mathrm{req} = \frac{25 \pm 9\,\mathrm{\mu g\,OOA\,sm^{-3}\,(ppmv\,CO)^{-1}}}{\mathrm{EF_{GPOM,CO}}(f_\mathrm{gas}, f_\mathrm{dies})} \tag{16}$$

where $\mathrm{FR}(f_\mathrm{gas}, f_\mathrm{dies})$ is the fraction of GPOM reacted (FR = Fraction Reacted) after 0.45 days of photochemical aging for a given fractional fuel usage. The predictions of Eq. (16) are shown in Fig. 3a. Note that, as a result of gasoline having a higher $\mathrm{EF_{CO}}$ and a lower $\mathrm{EF_{GPOM}}$ than its diesel counterpart, the required overall SOA mass yield increases as the fraction of gasoline increases. In other words, the emission ratio $\mathrm{EF_{GPOM}/EF_{CO}}$ decreases as the fraction of gasoline use increases, thereby requiring a greater fraction of the emitted GPOM to be converted to SOA to match observations at the Pasadena ground site. Also shown in Fig. 3a are the SOA mass yields predicted, Y_pred, based on the values reported by Gentner et al. (2012) as a function of fractional fuel usage, which are calculated as:

$$Y_{\mathrm{pred}} = \frac{Y_{\mathrm{gas}} \times \mathrm{EF}_{\mathrm{GPOM,gas}} \times f_{\mathrm{gas}} + Y_{\mathrm{dies}} \times \mathrm{EF}_{\mathrm{GPOM,dies}} \times f_{\mathrm{dies}}}{\mathrm{EF}_{\mathrm{GPOM,gas}} \times f_{\mathrm{gas}} + \mathrm{EF}_{\mathrm{GPOM,dies}} \times f_{\mathrm{dies}}} \qquad (17)$$

where $Y_{\mathrm{gas}} = 0.023 \pm 0.007$ and $Y_{\mathrm{dies}} = 0.15 \pm 0.05$. As shown in Fig. 3a, the required and predicted yields match if the fuel usage is 3 % gasoline and 97 % diesel, and the propagated error-bars intersect when the fuel usage is 40 % gasoline and 60 % diesel, both of which are far from the reported fuel usage of 87 % gasoline and 13 % diesel. For reference, the closest any county in California comes to the required fuel usage is Glenn County (Northern California) which had fuel sales that were 58 % gasoline and 42 % diesel.

3.2 Potential explanations

3.2.1 Emission factor uncertainty

Given the discrepancy between predictions and observations of aggregate SOA mass yields shown in Fig. 3a, one deduces that for SOA predictions and observations to match (i.e. for the black and green lines in Fig. 3a to cross at $f_{\mathrm{gas}} = 0.87$), (1) the predicted aggregate SOA mass yield (green line) must be higher, or (2) the required SOA mass yield (black line) must be lower, or both (1) and (2) are true. One way by which the required composite SOA mass yield decreases is via an overall increase in the ratio of $\mathrm{EF}_{\mathrm{GPOM}}/\mathrm{EF}_{\mathrm{CO}}$, either by reducing $\mathrm{EF}_{\mathrm{CO}}$ and/or increasing $\mathrm{EF}_{\mathrm{GPOM}}$. To assess the accuracy of the emission factors reported in Gentner et al. (2012), we consider those reported in Fujita et al. (2012), given in Table 2. During August 2010, Fujita et al. (2012) measured emission factors for CO and total (products of incomplete combustion + non-combusted hydrocarbons + evaporative emissions) non-methane hydrocarbons (NMHC) obtained from tunnel measurements in Van Nuys, California, which is ~ 32 km west of the Pasadena ground site. Based on the results presented in Fujita et al. (2012) (Table 2), emission ratios measured in the Van Nuys tunnel range from 52.5 to 164 µg

NMHC sm^{-3} (ppmvCO)$^{-1}$, with an average value of 97.5 µg NMHC sm^{-3} (ppmvCO)$^{-1}$. Similarly to Gentner et al. (2012); Fujita et al. (2012) derived these fleet-average emission factors from vehicles traveling through a tunnel at near-constant speeds of approximately 40 mph, and excluded cold-start emissions, idle emissions, and diurnal and hot-soak evaporative hydrocarbon emissions. The Gentner et al. (2012) value is consistent with the lower end of the values reported in Fujita et al. (2012). The spread of values reported by Fujita et al. (2012) is most likely attributable to the fact that the emission factors derived include products of incomplete combustion and evaporative emissions during stabilized running conditions.

We examine the sensitivity of the required composite SOA mass yield by increasing the EF$_{\mathrm{GPOM,gas}}$ reported by Gentner et al. (2012) by a factor of 2.35, which increases the total EF$_{\mathrm{GPOM,CO}}$ given by Eq. (13) by a factor of 2 (increasing EF$_{\mathrm{GPOM,CO}}$ from 48.9 to 98.3 µg GPOM sm^{3} (ppmvCO)$^{-1}$ at 87 % gasoline and 13 % diesel) to match the mean value reported by Fujita et al. (2012) (Fig. 3b). As shown in Fig. 3b, increasing EF$_{\mathrm{GPOM,gas}}$ by a factor of 2.35 reduces the required SOA mass yields. However, this also reduces the predicted yields, since the SOA yield from pure gasoline is lower and since the gasoline terms in Eq. (17) have a larger impact than the diesel terms. The net result is that the required and predicted yields still match if the fuel usage is 3 % gasoline and 97 % diesel, and the propagated error-bars still intersect when the fuel usage is 40 % gasoline and 60 % diesel. Note that if the EF$_{\mathrm{GPOM,gas}}$ were increased even further, the predicted yield (Eq. 17) would asymptotically approach Y_{gas} and the required yield would approach zero (Eq. 16). In this analysis, we have assumed the evaporative emissions and products of incomplete combustion have the same SOA mass yield as the tail-pipe exhaust emissions. However, evaporative emissions will be enriched in small alkanes under ambient conditions. According to Fig. 2 of Gentner et al. (2012), the SOA mass yield of evaporative emissions is expected to be lower than tail-pipe emissions by a factor of ~ 10. Therefore, this analysis represents a conservative upper limit since evaporative emissions and products of incomplete combustion are not expected to contribute substantially to the SOA budget.

McDonald et al. (2013) recently assessed long-term trends (1990–2010) in $EF_{GPOM,CO}$ emission ratios for several US urban areas. As shown in Fig. 3b of McDonald et al. (2013), owing to differences in driving conditions and engine loads, the $EF_{GPOM,CO}$ emission ratios derived from tunnel measurements such as those of Gentner et al. (2012) and Fujita et al. (2012) may be lower than those derived from on-road studies in Los Angeles by a factor of 2.7. Therefore, to determine the upper limit of $EF_{GPOM,CO}$ that should be used in this analysis, we increase the overall (gas + diesel) $EF_{GPOM,CO}$ (Eq. 13) by a factor of 2.7. Doing so reduces the required yield (Eq. 14) by a factor of 0.37 ($Y_{req} = 0.37 \times 108.7\,\% = 40.2\,\%$). As shown in Fig. 3c, when the overall $EF_{GPOM,CO}$ is increased by a factor of 2.7, the predicted and required yields match if the fuel usage is 35 % gasoline and 65 % diesel, and the propagated uncertainties intersect if the fuel usage is 65 % gasoline and 35 % diesel.

Given the lack of agreement between predicted and required SOA mass yields (Fig. 3) when using the emission ratios from Fujita et al. (2012); Gentner et al. (2012) and McDonald et al. (2013), in order for vehicular emissions to make a significant contribution to the measured anthropogenic fossil OOA budget, at least one of the following must be true: (1) vehicular emission rates of gas-phase organic mass (relative to CO) are substantially larger than those recently measured; or (2) the SOA mass yields of pure gasoline and pure diesel exhaust are substantially (i.e. a factor of ∼ 3–16) higher than what has been measured previously. In the next section, we explore possibility (1) in the context of drive-cycle phases (e.g. cold-start emissions, idle emissions, hot-soak evaporative emissions, diurnal evaporative emissions, etc.) that were excluded from the development of the emission factors reported by Gentner et al. (2012) and used in this study.

3.2.2 Emission ratios from other drive-cycle phases

By sampling emissions within urban tunnels for sufficient periods of time, Fujita et al. (2012) and Gentner et al. (2012) estimated average emission factors. However, neither study included emissions from drive-cycle phases other than stabilized running in the emission factors used in this study. To estimate the impact of drive-cycle phase on emission-factor ratio, we use the California EMission FACtor model (EMFAC2011, http://www.arb.ca.gov/emfac/) combined with summer 2010 data for the South Coast Air Basin of California. Emission factors are weighted and aggregated by vehicle-year populations and speed distributions, and include all drive-cycle components (i.e. running, idle, start, diurnal evaporative, hot-soak evaporative, running evaporative, and resting evaporative). Emission factor ratios, based on daily-average emission rates, for all EMFAC2011 gasoline and diesel vehicle types are given in Tables 3 and 4, respectively. As shown in Table 3, EMFAC2011 predicts gasoline emission-factor ratios that are generally consistent with the values reported by Fujita et al. (2012) and are ~ 2–3.5 times higher than the value reported by Gentner et al. (2012). Based on the results shown in Fig. 3b, increasing the gasoline emission-factor ratio by ~ 2.5 reduces both the predicted and required SOA mass yields, which does not improve agreement. As shown in Table 4, the diesel emission-factor ratios predicted by EMFAC2011 are very similar to the value reported by Gentner et al. (2012). These results show that the required and predicted yields do not match even if all drive-cycle phases are accounted for. Therefore, one concludes that either the SOA mass yields for gasoline and diesel exhaust are significantly higher than what has been previously reported, or non-vehicular source categories contribute significantly to the anthropogenic fossil OOA budget measured at the Pasadena ground site. Both of these possibilities are explored in the next section.

3.2.3 Ambient NMHC/ΔCO ratios

The analysis up to this point has been based on measured and predicted NMHC/CO vehicular emission ratios and measured ambient OOA/ΔCO ratios at the Pasadena ground site. This analysis is now extended to include all upwind NMHC source categories (vehicular and non-vehicular) by comparing measured ambient NMHC/ΔCO ratios to measured ambient OOA/ΔCO at the Pasadena ground site. The four main source categories of NMHC in Southern California, not including trans-Pacific transport, which is thought to be unimportant for SOA formation in the L.A. Basin due to long transport times and intense dilution, are stationary, areawide, mobile, and natural (non-fossil). Based on the 2009 Almanac Emission Projection Data reported by the CARB (http://www.arb.ca.gov/app/emsinv/emssumcat.php), the 2010 annual emissions of reactive organic gas (ROG) and CO from each source are given in Table 5. Note that CARB reports ROG emission rates, which are similar to NMHC but do not include several low-reactive organic compounds such as ethane, acetone, CFCs, and HCFCs. As shown in Table 5, on-road motor vehicles are reported to contribute ~ 27–29 % of all ROG emissions in the South Coast Air Basin and Los Angeles County. Mobile sources other than on-road vehicles (e.g. aircraft, trains, ocean-going vessels, and off-road equipment such as fork-lifts) are reported to contribute ~ 21 % of the ROG emissions.

Figure 4 shows two lumped NMHC concentrations (e.g. single-ring aromatics and small alkanes), normalized by ΔCO, as functions of photochemical age. See Table 6 for a list of all compounds included in Fig. 4. As shown in Fig. 4, similarly to the roughly linear increases in OOA/ΔCO with increasing photochemical age, gas-phase alkane (C_6, C_9–C_{11}) and single-ring aromatic concentrations both exhibit roughly linear decreases with increasing photochemical age. Note that adding the normalized alkanes and single-ring aromatic concentrations at zero photochemical age suggests an emission ratio of ~ $55\,\mu g\,GPOM\,sm^{-3}\,(ppmvCO)^{-1}$, which is similar to the estimated emission ratio given by Eq. (13). Although this is not proof, the linear decrease in normalized NMHC concentrations with photochemical age, and the similarity between estimated emission ratios are both consistent with vehicular exhaust being the dominant source of these compounds. Furthermore, in contrast to the numbers given in Table 5, Borbon et al. (2013) found that emissions from gasoline-powered vehicles dominated the urban anthropogenic NMHC budget during CalNex.

One particularly interesting feature of Fig. 4 is that even if all upwind sources of linear alkanes (C_6, C_9–C_{11}) and single-ring aromatics are accounted for, the required aggregate SOA mass yield is still ~ 92 % (92 = OOA/ΔCO slope divided by negative

NMHC/ΔCO slope = 57/62). This required yield may be overestimated because only light straight-chain (C_6, C_9–C_{11}) alkane and single-ring aromatic ($< C_{12}$) concentration measurements are available, whereas the majority of alkanes in the ambient are expected to be branched (Fig. 2c). That being said, the required yield of 92 % is still inexplicably large considering that the single-ring aromatic component of vehicular exhaust is expected to produce ∼ 2.5 times more SOA than the alkane component (Fig. 2c). A similar correspondence between the magnitude of aromatic hydrocarbon decreases and SOA increases was observed by de Gouw et al. (2005) in the 2002 New England Air Quality Study. It is possible that alkanes and aromatics with 12 or more carbon atoms are contributing to the SOA budget. However, alkanes and aromatics ($\geq C_{12}$) attributable to vehicular activity are abundant only in diesel exhaust, and not in gasoline exhaust. If alkanes ($\geq C_{12}$) were contributing substantially to the L.A. SOA budget, one would expect to see a significant decrease in OOA concentrations on the weekends when diesel activity is reduced by ∼ 50 %. However, this possibility is not supported by the conclusions of Hayes et al. (2013) and Bahreini et al. (2012), or the emission ratio analysis presented in this study.

4 Conclusions

Using the best available laboratory-derived SOA mass yields, the SV-OOA/ΔCO enhancements attributable to anthropogenic fossil activity (Fig. 1) cannot be explained by the measured and predicted NMHC/CO vehicular emission ratios or the measured ambient NMHC/ΔCO ratios. This conclusion is based on the following observations:

- Emission factors and estimated yields reported in Gentner et al. (2012); Fujita et al. (2012); McDonald et al. (2013) and calculated using EMFAC2011 significantly underpredict OOA/ΔCO enhancements when compared to CalNex observations.

- Accounting for emissions from all drive-cycle phases (e.g. start, idle, evaporative, running, etc.) does not improve agreement between predicted and required SOA mass yields significantly.
- Accounting for all upwind sources of single-ring aromatics and light alkanes (C_6, C_9–C_{11}) does not improve agreement between predicted and required SOA mass yields significantly.

We return to the question: "Is it more likely that (1) ambient SOA mass yields are substantially (i.e. a factor of $\sim$ 3–16, best estimate is 7.4, Fig. 3c) larger than what has been derived experimentally, or (2) vehicular emissions do not dominate SOA concentrations attributable to anthropogenic fossil activity in Southern California?". The answer may, in fact, involve both of these two possibilities. Therefore, both options should be explored further, particularly since their implications for SOA control strategies are markedly different.

Acknowledgements. The authors would like to thank Roya Bahreini, Drew Gentner, Arthur Chan, and Allen Goldstein for very useful comments. This work was supported by NOAA grant NA13OAR4310058. PLH and JLJ thank CARB 08-309 &11-305, DOE (BER/ASR) DE-SC0006035, and a CIRES Visiting Fellowship.

References

Aiken, A. C., DeCarlo, P. F., Kroll, J. H., Worsnop, D. R., Huffman, J. A., Docherty, K. S., Ulbrich, I. M., Mohr, C., Kimmel, J. R., Sueper, D., Sun, Y., Zhang, Q., Trimborn, A., Northway, M., Ziemann, P. J., Canagaratna, M. R., Onasch, T. B., Alfarra, M. R., Prevot, A. S. H., Dommen, J., Duplissy, J., Metzger, A., Baltensperger, U., and Jimenez, J. L.: O/C and OM/OC ratios of primary, secondary, and ambient organic aerosols with high-resolution time-of-flight aerosol mass spectrometry, Environ. Sci. Technol., 42, 4478–4485, 2008. 27783

Atkinson, R. J.: Gas-phase tropospheric chemistry of volatile organic compounds: 1. alkanes and alkenes, Phys. Chem. Ref. Data, 26, 215–290, 1997. 27801

Bahreini, R., Middlebrook, A. M., de Gouw, J. A., Warneke, C., Trainer, M., Brock, C. A., Stark, H., Brown, S. S., Dube, W. P., Gilman, J. B., Hall, K., Holloway, J. S., Kuster, W. C., Perring, A. E., Prevot, A. S. H., Schwarz, J. P., Spackman, J. R., Szidat, S., Wagner, N. L., Weber, R. J., Zotter, P., and Parrish, D. D.: Gasoline emissions dominate over diesel in formation of secondary organic aerosol mass, Geophys. Res. Lett., 39, L06805, doi:10.1029/2011GL050718, 2012. 27781, 27782, 27784, 27787, 27794

Borbon, A., Gilman, J. B., Kuster, W. C., Grand, N., Chevaillier, S., Colomb, A., Dolgorouky, C., Gros, V., Lopez, M., Sarda-Esteve, R., Holloway, J. S., Stutz, J., Petetin, H., McKeen, S., Beekmann, M., Warneke, C., Parrish, D. D., and de Gouw, J. A.: Emission ratios of anthropogenic volatile organic compounds in northern mid-latitude megacities: observations vs. emission inventories in Los Angeles and Paris, J. Geophys. Res.-Atmos., 118, 2041–2057, 2013. 27793

California Air Resources Board: Motor Vehicle Emission Factor/Emission Inventory Model – EMFAC 2011, available at: http://www.arb.ca.gov/msei/msei.htm (last access: 20 June 2013), 2011.

Calvert, J. G., Atkinson, R., Becker, K. H., Kamens, R. M., Seinfeld, J. H., Wallington, T. J., and Yarwood, G.: The Mechanisms of Atmospheric Oxidation of Aromatic Hydrocarbons, Oxford University Press, New York, 556 pp., 2002. 27801

DeCarlo, P. F., Kimmel, J. R., Trimborn, A., Northway, M. J., Jayne, J. T., Aiken, A. C., Gonin, M., Fuhrer, K., Horvath, T., Docherty, K. S., Worsnop, D. R., and Jimenez, J. L.: Field-deployable, high-resolution, time-of-flight aerosol mass spectrometer, Anal. Chem., 78, 8281–8289, 2006. 27783

de Gouw, J. A., Middlebrook, A. M., Warneke, C., Goldan, P. D., Kuster, W. C., Roberts, J. M., Fehsenfeld, F. C., Worsnop, D. R., Canagaratna, M. R., Pszenny, A. A. P., Keene, W. C., Marchewka, M., Bertman, S. B., and Bates, T. S.: Budget of organic carbon in a polluted atmosphere: Results from the New England Air Quality Study in 2002, J. Geophys. Res.-Atmos., 110, D16305, doi:10.1029/2004JD005623 2005. 27781, 27794

de Gouw, J. A., Brock, C. A., Atlas, E. L., Bates, T. S., Fehsenfeld, F. C., Goldan, P. D., Holloway, J. S., Kuster,Lerner, B. M., Matthew, B. M., Middlebrook, A. M., Onasch, T. B., Peltier, R. E., Quinn, P. K., Senff, C. J., Stohl, A., Sullivan, A. P., Trainer, M., Warneke, C., Weber, R. J., and Williams, E. J.: Sources of particulate matter in the northeastern United States: 1. Direct emissions and secondary formation of organic matter in urban plumes, J. Geophys. Res.-Atmos., 113, D08301, doi:10.1029/2007JD009243, 2008. 27781 de Gouw, J. A., Gilman, J. B., Borbon, A., Warneke, C., Kuster, W. C., Goldan, P. D., Holloway, J. S., Peischl, J., Ryerson, T. B., Parrish, D. D., Gentner, D. R., Goldstein, A. H., and Harley, R. A.: Increasing atmospheric burden of ethanol in the United States, Geophys. Res. Lett., 39, L15803, doi:10.1029/2012GL052109, 2012.

Dusanter, S., Vimal, D., Stevens, P. S., Volkamer, R., and Molina, L. T.: Measurements of OH and HO_2 concentrations during the MCMA-2006 field campaign – Part 1: Deployment of the Indiana University laser-induced fluorescence instrument, Atmos. Chem. Phys., 9, 1665–1685, doi:10.5194/acp-9-1665-2009, 2009. 27782

Fujita, E. M., Campbell, D. E., Zielinska, B., Chow, J. C., Lindhjem, C. E., DenBleyker, A., Bishop, G. A., Schuchmann, B. G., Stedman, D. H., and Lawson, D. R.,: Comparison of the MOVES2010a, MOBILE6.2, and EMFAC2007 mobile source emission models with on-road traffic tunnel and remote sensing measurements, J. Air Waste Manag., 62, 1134–1149, 2012. 27789, 27790, 27791, 27792, 27794, 27802

Gentner, D. R., Isaacman, G., Worton, D. R., Chan, A. W. H., Dallmann, T. R., Davis, L., Liu, S., Day, D. A., Russell, L. M., Wilson,Weber, R., Uha, A., Harley, R. A., and Goldstein, A. H.: Elucidating secondary organic aerosol from diesel and gasoline vehicles through detailed characterization of organic carbon emissions, P. Natl. Acad. Sci. USA, 109, 18318–18323, 2012. 27781, 27784, 27785, 27786, 27787, 27788, 27789, 27790, 27791, 27792, 27794, 27802, 27803, 27804, 27808, 27809

Gerbig, C., Schmitgen, S., Kley, D., Volz-Thomas, A., Dewey, K., and Haaks, D.: An improved fast-response vacuum-UV resonance fluorescence CO instrument, J. Geophys. Res.-Atmos., 104, 1699–1704, 1999. 27782

Gilman, J. B., Kuster, W. C., Goldan, P. D., Herndon, S. C., Zahniser, M. S., Tucker, S. C., Brewer, W. A., Lerner, B. M., Williams, E. J., Harley, R. A., Fehsenfeld, F. C., Warneke, C., and de Gouw, J. A.: Measurements of volatile organic compounds during the 2006 TexAQS/GoMACCS campaign: industrial influences, regional characteristics, and diurnal dependencies of the OH reactivity, J. Geophys. Res.-Atmos., 114, D00F06, doi:10.1029/2008JD011525 2009. 27783

Hayes, P. L., Ortega, A. M., Cubison, M. J., Froyd, K. D., Zhao, Y., Cliff, S. S., Hu, W. W., Toohey, D. W., Flynn, J. H., Lefer, B. L., Grossberg, N., Alvarez, S., Rappengluck, B., Taylor, J. W., Allan, J. D., Holloway, J. S., Gilman, J. B., Kuster, W. C., de Gouw, J. A., Massoli, P., Zhang, X., Liu, J., Weber, R. J., Corrigan, A. L., Russell, L. M., Isaacman, G., Worton, D. R., Kreisberg, N. M., Goldstein, A. H., Thalman, R., Waxman, E. M., Volkamer, R., Lin, Y. H., Surratt, J. D., Kleindienst, T. E., Offenberg, J. H., Dusanter, S., Griffith, S., Stevens, P. S., Brioude, J., Angevine, W. M., Jimenez, J. L.: Organic aerosol composition and sources in Pasadena, California during the 2010 CalNex Campaign, J. Geophys. Res.-Atmos., 118, 9233–9257, doi:10.1002/jgrd.50530, 2013. 27781, 27782, 27783, 27787, 27794, 27807

Hodzic, A., Jimenez, J. L., Madronich, S., Canagaratna, M. R., DeCarlo, P. F., Kleinman, L., and Fast, J.: Modeling organic aerosols in a megacity: potential contribution of semi-volatile and intermediate volatility primary organic compounds to secondary organic aerosol formation, Atmos. Chem. Phys., 10, 5491–5514, doi:10.5194/acp-10-5491-2010, 2010.

Johnson, D., Utembe, S. R., Jenkin, M. E., Derwent, R. G., Hayman, G. D., Alfarra, M. R., Coe, H., and McFiggans, G.: Simulating regional scale secondary organic aerosol formation during the TORCH 2003 campaign in the southern UK, Atmos. Chem. Phys., 6, 403–418, doi:10.5194/acp-6-403-2006, 2006. 27781

Jimenez, J. L., Canagaratna, M. R., Donahue, N. M., Prevot, A. S. H., Zhang, Q., Kroll, J. H., DeCarlo, P. F., Allan, J. D., Coe, H., Ng, N. L., Aiken, A. C., Docherty, K. S., Ulbrich, I. M., Grieshop, A. P., Robinson, A. L., Duplissy, J., Smith, J. D., Wilson, K. R., Lanz, V. A., Hueglin, C., Sun, Y. L., Tian, J., Laaksonen, A., Raatikainen, T., Rautiainen, J., Vaattovaara, P., Ehn, M., Kulmala, M., Tomlinson, J. M., Collins, D. R., Cubison, M. J., Dunlea, E. J., Huffman, J. A., Onasch, T. B., Alfarra, M. R., Williams, P. I., Bower, K., Kondo, Y., Schneider, J., Drewnick, F., Borrmann, S., Weimer, S., Demerjian, K., Salcedo, D., Cottrell, L., Griffin, R., Takami, A., Miyoshi, T., Hatakeyama, S., Shimono, A., Sun, J. Y., Zhang, Y. M., Dzepina, K., Kimmel, J. R., Sueper, D., Jayne, J. T., Herndon, S. C., Trimborn, A. M., Williams, L. R., Wood, E. C., Middlebrook, A. M., Kolb, C. E., Baltensperger, U., and Worsnop, D. R.: Evolution of organic aerosols in the atmosphere, Science, 326, 1525–1529, 2009. 27783

Kleinman, L. I., Springston, S. R., Daum, P. H., Lee, Y.-N., Nunnermacker, L. J., Senum, G. I., Wang, J., Weinstein-Lloyd, J., Alexander, M. L., Hubbe, J., Ortega, J., Canagaratna, M. R., and Jayne, J.: The time evolution of aerosol composition over the Mexico City plateau, Atmos. Chem. Phys., 8, 1559–1575, doi:10.5194/acp-8-1559-2008, 2008. 27781, 27783

Matsui, H., Koike, M., Takegawa, N., Kondo, Y., Griffin, R. J., Miyazaki, Y., Yokouchi, Y., and Ohara, T.: Secondary organic aerosol formation in urban air: temporal variations and possible contributions from unidentified hydrocarbons, J. Geophys. Res.-Atmos., 114, D04201, doi:10.1029/2008JD010164, 2009. 27781

McDonald, B. C., Gentner, D. R., Goldstein, A. H., and Harley, R. A.: Long-term trends in motor vehicle emissions in US urban areas, Environ. Sci. Technol., 47, 10022–10031, doi:10.1021/es401034z, 2013. 27786, 27791, 27794, 27809

Paatero, P. and Tapper, U.: Positive matrix factorization – a nonnegative factor model with optimal utilization of error-estimates of data values, Environmetrics, 5, 111–126, 1994. 27783

Parrish, D. D., Stohl, A., Forster, C., Atlas, E. L., Blake, D. R., Goldan, P. D., Kuster, W. C., and de Gouw, J. A.: Effects of mixing on evolution of hydrocarbon ratios in the troposphere, J. Geophys. Res.-Atmos., 112, D10S34, doi:10.1029/2006JD007583, 2007. 27783, 27807

Ryerson, P. L., Andrews, A. E., Angevine, W. M., Bates, T. S., Brock, C. A., Cairns, B., Cohen, R. C., Cooper, O. R., de Gouw, J. A., Fehsenfeld, F. C., Ferrare, R. A., Fischer, M. L., Flagan, R. C., Goldstein, A. H., Hair, J. W., Hardesty, R. M., Hostetler, C. A., Jimenez, J. L., Langford, A. O., McCauley, E., McKeen, S. A., Molina, L. T., Nenes, A., Oltmans, S. J., Parrish, D. D., Pederson, J. R., Pierce, R. B., Prather, K., Quinn, P. K., Seinfeld, J. H., Senff, C. J., Sorooshian, A., Stutz, J., Surratt, J. D., Trainer, M., Volkamer, R., Williams, E. J., and Wofsy, S. C.: The 2010 California Research at the Nexus of Air Quality and Climate Change (CalNex) field study, J. Geophys. Res. Atmos., 118, 5830–5866, doi:10.1002/jgrd.50331, 2013. 27781, 27782

Thalman, R. and Volkamer, R.: Inherent calibration of a blue LED-CE-DOAS instrument to measure iodine oxide, glyoxal, methyl glyoxal, nitrogen dioxide, water vapour and aerosol extinction in open cavity mode, Atmos. Meas. Tech., 3, 1797–1814, doi:10.5194/amt-3-1797-2010, 2010. 27783

Ulbrich, I. M., Canagaratna, M. R., Zhang, Q., Worsnop, D. R., and Jimenez, J. L.: Interpretation of organic components from Positive Matrix Factorization of aerosol mass spectrometric data, Atmos. Chem. Phys., 9, 2891–2918, doi:10.5194/acp-9-2891-2009, 2009. 27783

Volkamer, R., Jimenez, J. L., San Martini, F., Dzepina, K., Zhang, Q., Salcedo, D., Molina, L. T., Worsnop, D. R., and Molina, M. J.: Secondary organic aerosol formation from anthropogenic air pollution: rapid and higher than expected, Geophys. Res. Lett., 33, L17811, doi:10.1029/2006GL026899, 2006. 27781

Warneke, C., deGouw, J. A., Holloway, J. S., Peischl, J., Ryerson, T. B., Atlas, E., Blake, D., Trainer, M., and Parrish, D. D: Multiyear trends in volatile organic compounds in Los Angeles, California: five decades of decreasing emissions, J. Geophys. Res.-Atmos., 117, D00V17, doi:10.1029/2012JD017899, 2012. 27781

Zhang, Q., Jimenez, J. L., Canagaratna, M. R., Allan, J. D., Coe, H., Ulbrich, I., Alfarra, M. R., Takami, A., Middlebrook, A. M., Sun, Y. L., Dzepina, K., Dunlea, E., Docherty, K., DeCarlo, P. F., Salcedo, D., Onasch, T., Jayne, J. T., Miyoshi, T., Shimono, A., Hatakeyama, S., Takegawa, N., Kondo, Y., Schneider, J., Drewnick, F., Borrmann, S., Weimer, S., Demerjian, K., Williams, P., Bower, K., Bahreini, R., Cottrell, L., Griffin, R. J., Rautiainen, J., Sun, J. Y., Zhang, Y. M., and Worsnop, D. R.: Ubiquity and dominance of oxygenated species in organic aerosols in anthropogenically-influenced Northern Hemisphere mid-latitudes, Geophys. Res. Lett., 34, L13801, doi:10.1029/2007GL029979, 2007b. 27783

Zotter, P., El-Haddad, I., Zhang, Y., Hayes, P. L., Zhang, X., Lin, Y., Wacker, L., Schnelle-Kreis, J., Abbaszade, G., Zimmermann, R., Surratt, J. D., Weber, R., Jimenez, J. L., Szidat, S., Baltensperger, U., and Prevot, A. S. H.: Diurnal cycle of fossil and non-fossil carbon using radiocarbon analyses during CalNex, Atmos. Chem. Phys. Discuss., submitted, 2013. 27784

Table 1. Fraction of hydrocarbon reacted for an OH-exposure = 58.3×10^9 molec cm^{-3} s at 298 K and 1 atm. Hydrocarbons shown are abundant in a typical mixture of liquid gasoline and diesel fuel. Fraction reacted = $1 - \exp(-k_{OH} \times [OH] \times t)$.

Hydrocarbon	Fraction Reacted	OH reaction-rate constant (cm^3 molec^{-1} s^{-1})
benzene[a]	0.069	1.22×10^{-12}
toluene[a]	0.280	5.63×10^{-12}
m-xylene[a]	0.740	2.31×10^{-11}
n-hexane[b]	0.272	5.45×10^{-12}
n-octane[b]	0.398	8.71×10^{-12}
n-dodecane[b]	0.555	1.39×10^{-11}

[a] Reaction rate constants from Calvert et al. (2002).

[b] Reaction rate constants from Atkinson (1997).

Table 2. Measured fleet-averaged fuel-based CO and NMHC emission factors (g kg^{-1} of fuel) reported by Fujita et al. (2012); Gentner et al. (2012). Numerical values in the right-most column are calculated using the conversion factor 1250 µg CO sm^{-3} (ppmvCO)$^{-1}$.

Date Values from Fujita et al. (2012)	Temperature °F	EF_{CO} $\frac{\text{g CO}}{\text{kg fuel}}$	EF_{NMHC} $\frac{\text{g NMHC}}{\text{kg fuel}}$	EF_{NMHC}/EF_{CO} $\frac{\text{g NHMC}}{\text{g CO}}$	EF_{NMHC}/EF_{CO} $\frac{\mu\text{g NMHC sm}^{-3}}{\text{ppmv CO}}$
Aug 21, Sat PM	95	23.0	1.59	0.069	86.3
Aug 22, Sun PM	92	25.4	1.98	0.078	97.5
Aug 24, Tue AM	92	16.7	1.40	0.084	105
Aug 24, Tue PM	101	19.1	2.51	0.131	164
Aug 25, Wed AM	92	18.9	1.35	0.071	88.8
Aug 25, Wed PM	102	30.4	3.05	0.100	125
Aug 28, Sat AM	72	25.9	1.09	0.042	52.5
Aug 29, Sun AM	70	10.7	0.51	0.048	60.0
Mean		21.3	1.69	0.078	97.5
Median		21.1	1.50	0.075	93.8
Values from Gentner et al. (2012)				0.039	48.8

Table 3. Gasoline vehicle-specific emission ratios, EF_{NMHC}/EF_{CO}, predicted by EMFAC2011 (http://www.arb.ca.gov/emfac/) for the South Coast Air Basin in Summer 2010. Emission ratios are based on daily CO and NMHC emission rates calculated by EMFAC2011. Emission ratios include all drive-cycle components (i.e. running, idle, start, diurnal evaporative, hot-soak evaporative, running evaporative, and resting evaporative). Rows are ordered in descending population. Numerical values in $\frac{\mu g\,NMHC\,m^{-3}}{ppmv\,CO}$ columns are calculated using the conversion factor $1250\,\mu g\,CO\,sm^{-3}\,(ppmv\,CO)^{-1}$. Note that the values predicted by EMFAC are higher than what is reported by Gentner et al. (2012) because they include products of incomplete combustion, evaporative emissions, and start emissions.

Veh. Class[a]	$\frac{g\,NHMC}{g\,CO}$	$\frac{\mu g\,NMHC\,sm^{-3}}{ppmv\,CO}$	Population
Values from Gentner et al. (2012)	0.031	38.3	Caldecott Tunnel
LDA	0.116	145	5 566 383
LDT2	0.093	116	1 806 334
MDV	0.081	101	1 474 925
LDT1	0.112	140	655 343
LHD1	0.115	144	257 882
MCY	0.161	201	213 296
MH	0.035	43.8	58 258
LHD2	0.112	140	27 933
T6TS	0.096	120	22 177
OBUS	0.088	110	7278
UBUS	0.100	125	1766
T7IS	0.051	63.8	1501
SBUS	0.068	85.0	1491

[a] See http://www.arb.ca.gov/msei/emfac2011-pl-users-guide-122112.pdf for a detailed description of each vehicle class.

Table 4. Diesel vehicle-specific emission ratios, EF_{NMHC}/EF_{CO}, predicted by EMFAC2011 (http://www.arb.ca.gov/emfac/) for the South Coast Air Basin in Summer 2010. Emission ratios are based on daily CO and NMHC emission rates calculated by EMFAC2011. Emission ratios include all drive-cycle components (i.e. running, idle, start, diurnal evaporative, hot-soak evaporative, running evaporative, and resting evaporative). Rows are ordered in descending population. Numerical values in $\frac{\mu g\,NMHC\,m^{-3}}{ppmv\,CO}$ columns are calculated using the conversion factor $1250\,\mu g\,CO\,sm^{-3}\,(ppmvCO)^{-1}$

Veh. Class[a]	$\frac{g\,NHMC}{g\,CO}$	$\frac{\mu g\,NMHC\,m^{-3}}{ppmv\,CO}$	Population
Values from Gentner et al. (2012)	0.224	280.0	Caldecott Tunnel
LHD1	0.204	255	80 690
T6 instate small	0.256	320	37 131
LHD2	0.203	254	27 901
LDA	0.225	281	19 184
T6 instate heavy	0.275	344	15 303
T7 tractor	0.219	274	11 037
MH	0.261	326	10 110
T7 POLA	0.198	248	9,818
T7 Single	0.220	275	8,951
UBUS	0.217	271	7,084
T6 instate construction small	0.256	320	5,410
T7 NNOOS	0.224	280	5,372
T7 CAIRP	0.227	284	5,325
T6 Public	0.272	340	5,282
T7 SWCV	0.232	290	4,839
SBUS	0.314	393	4,388
T7 Public	0.267	334	3,579
All Other Buses	0.278	348	3,178
T7 single construction	0.220	275	3,176
T7 tractor construction	0.221	276	2,306
T6 instate construction heavy	0.275	344	2,242
T7 NOOS	0.231	289	1,939
MDV	0.205	256	1,504
Motor Coach	0.232	290	1,313
LDT1	0.236	295	953
T6 utility	0.238	298	890
LDT2	0.245	306	861
T7 utility	0.243	304	423
T7 CAIRP construction	0.227	284	392
T7 Ag	0.217	271	231
T6 Ag	0.291	364	187
T6 CAIRP small	0.244	305	136
T6 OOS small	0.244	305	78
T6 CAIRP heavy	0.258	323	44
T6 OOS heavy	0.258	323	25

[a] See http://www.arb.ca.gov/msei/emfac2011-pl-users-guide-122112.pdf for a detailed description of each vehicle class.

Table 5. CARB 2010 Estimated daily emission rates (annual average). Units are (metric-tons day^{-1}).

Source	Los Angeles County		South Coast Air Basin	
	CO	ROG[a]	CO	ROG[a]
STATIONARY SOURCES				
FUEL COMBUSTION	24.1 (1.3 %)	4.3 (1.1 %)	34.1 (1.1 %)	5.8 (0.9 %)
WASTE DISPOSAL	0.8 (0 %)	0.9 (0.2 %)	1.1 (0 %)	9.1 (1.4 %)
CLEANING AND SURFACE COATINGS	0.0 (0 %)	25.8 (6.6 %)	0.1 (0 %)	40.7 (6.1 %)
PETROLEUM PRODUCTION AND MARKETING	8.9 (0.5 %)	25.1 (6.4 %)	8.9 (0.3 %)	33.2 (5.0 %)
INDUSTRIAL PROCESSES	1.3 (0 %)	11.6 (3.0 %)	2.5 (0 %)	20.2 (3.0 %)
TOTAL STATIONARY SOURCES	35.0 **(1.9 %)**	67.7 **(17.3 %)**	46.8 **(1.5 %)**	109.0 **(16.5)**
AREAWIDE SOURCES				
SOLVENT EVAPORATION	0 (0 %)	82.7 (21.2 %)	0 (0 %)	129.4 (19.5 %)
MISCELLANEOUS PROCESSES	51.2 (2.8 %)	5.4 (1.4 %)	112.3 (3.6 %)	14.7 (2.2 %)
TOTAL AREAWIDE SOURCES	51.2 **(2.8 %)**	88.0 **(22.5 %)**	112.3 **(3.6 %)**	144.1 **(21.8 %)**
MOBILE SOURCES				
ON-ROAD MOTOR VEHICLES	1096.3 (60.0 %)	113.1 (29.0 %)	1817.6 (58.4 %)	182.8 (27.6 %)
OTHER MOBILE SOURCES	579.5 (31.7 %)	81.0 (20.7 %)	973.2 (31.3 %)	140.1 (21.1)
TOTAL MOBILE SOURCES	1675.8 **(91.7 %)**	194.1 **(49.7 %)**	2790.8 **(89.6 %)**	322.9 **(48.7 %)**
NATURAL (NON-ANTHROPOGENIC) SOURCES				
NATURAL SOURCES	65.0 (3.6 %)	40.5 (10.4 %)	164.2 (5.3 %)	86.5 (13.1 %)
TOTAL NATURAL SOURCES	65.0 **(3.6 %)**	40.5 **(10.4 %)**	164.2 **(5.3 %)**	86.5 **(13.1 %)**

(http://www.arb.ca.gov/app/emsinv/emssumcat.php)

[a] CARB reports ROG emission rates, which are similar to NMHC but do not include several low-reactive organic compounds such as ethane, acetone, CFCs, and HCFCs.

Table 6. Chemical constituents of lumped species shown in Fig. 4.

Alkanes (C_6,C_9-C_{11})	Single-ring aromatics
n-hexane	benzene
n-nonane	toluene
n-decane	o-xylene
n-undecane	m-xylene
	p-xylene
	1-ethyl benzene
	styrene
	isopropyl benzene
	npropyl benzene
	1-ethyl 2-methyl benzene
	1-ethyl 3-methyl benzene
	1-ethyl 4-methyl benzene
	1,2,3-trimethylbenzene
	1,2,4-trimethylbenzene
	1,3,5-trimethylbenzene

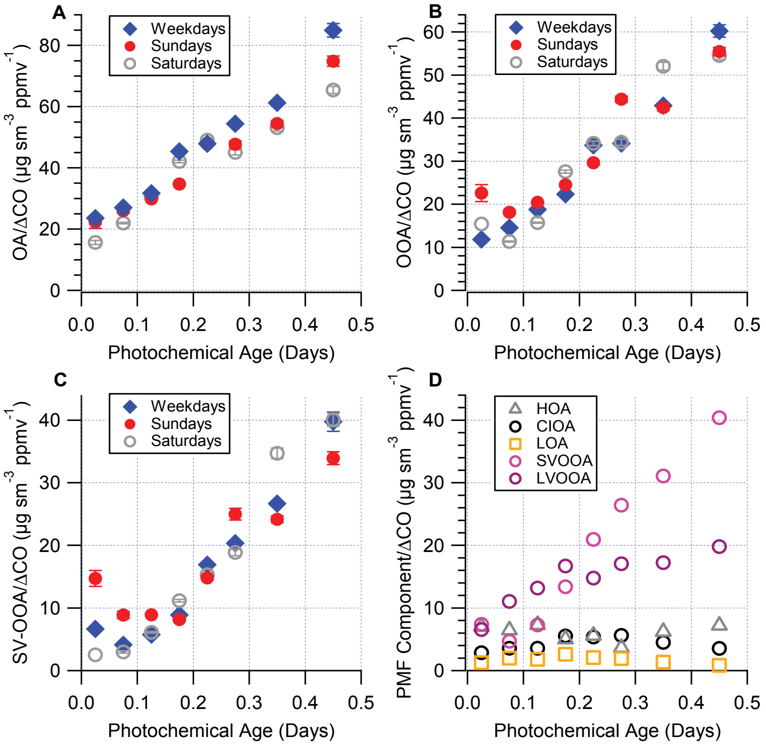

Fig. 1. Measured AMS PMF factor concentrations normalized by CO enhancement ΔCO is the ambient CO minus the estimated background CO (105 ppb) as functions of photochemical age (see Hayes et al., 2013, for a detailed description of how this figure was constructed). **(A)** The evolution of OA/ΔCO vs. photochemical age for Pasadena during CalNex separated by day of the week. Error bars indicate the standard errors. Photochemical age is determined using the method of Parrish et al. (2007). Also shown are the analogous plots for **(B)** OOA and **(C)** SV-OOA. **(D)** Evolution of the PMF component concentrations normalized to ΔCO vs. photochemical age.

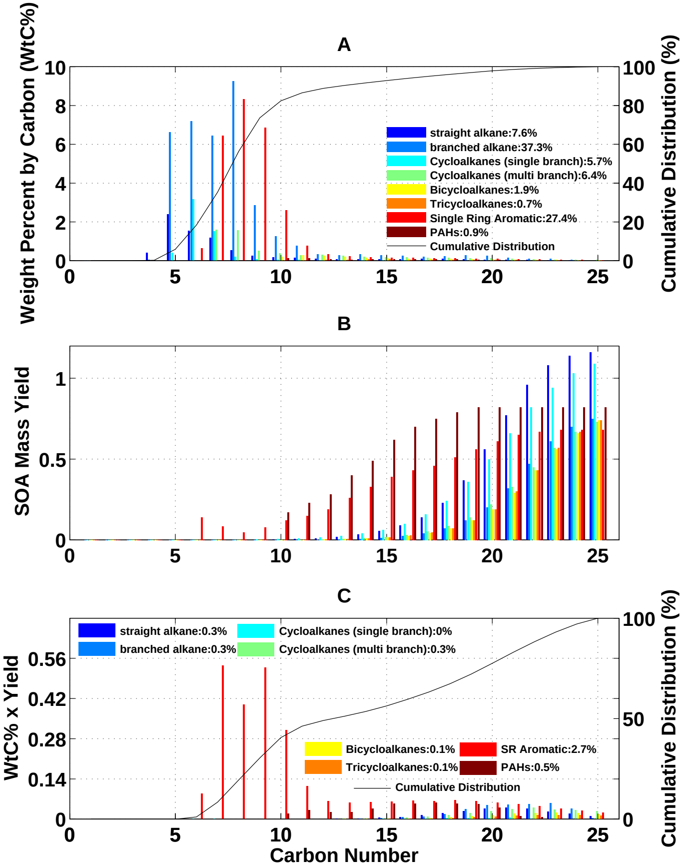

Fig. 2. Distribution of mass by chemical class based on California fuel-sale data comprising 13 % diesel and 87 % gasoline, by volume (top panel). Distribution of compound specific SOA mass yields (middle panel). Relative contributions of each group of species to predicted SOA, calculated as the yields multiplied by weight percent (by carbon) in liquid fuel (bottom panel). Data are from Tables S5, S6, and S8 of Gentner et al. (2012).

Title Page
Abstract
Introduction
Conclusions
References
Tables
Figures
◀︎I
▶︎I
◀︎
▶︎
Back
Close
Full Screen / Esc
Printer-friendly Version
Interactive Discussion

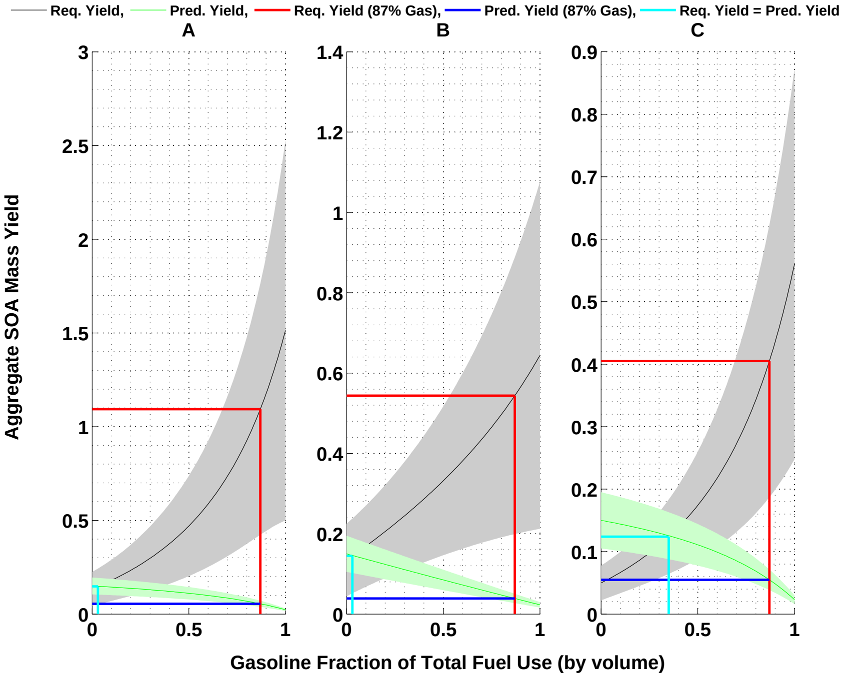

Fig. 3. Predicted and Required SOA mass yields. **(A)** Black line: aggregate SOA mass yields required to match observations at the Pasadena ground site as a function of gasoline and diesel fuel sales (by volume). Green line: yield predicted by Gentner et al. (2012) as a function of gasoline and diesel fuel sales (by volume). Red line: yield required for 87 % gasoline and 13 % diesel fuel (state-average). Blue line: yield predicted by Gentner et al. (2012) for 87 % gasoline and 13 % diesel fuel (state-average). Cyan line: point at which the black line crosses the green line. **(B)** Same as **(A)** except $EF_{GPOM,gas}$ have been increased by a factor of 2.35. **(C)** Same as **(A)** except $EF_{GPOM,gas}$ and $EF_{GPOM,dies}$ have both been increased by a factor of 2.7 (McDonald et al., 2013). Error-bars correspond to propagated uncertainties, and all plots have been adjusted to account for partial reaction of hydrocarbons at 0.45 days of photochemical aging.

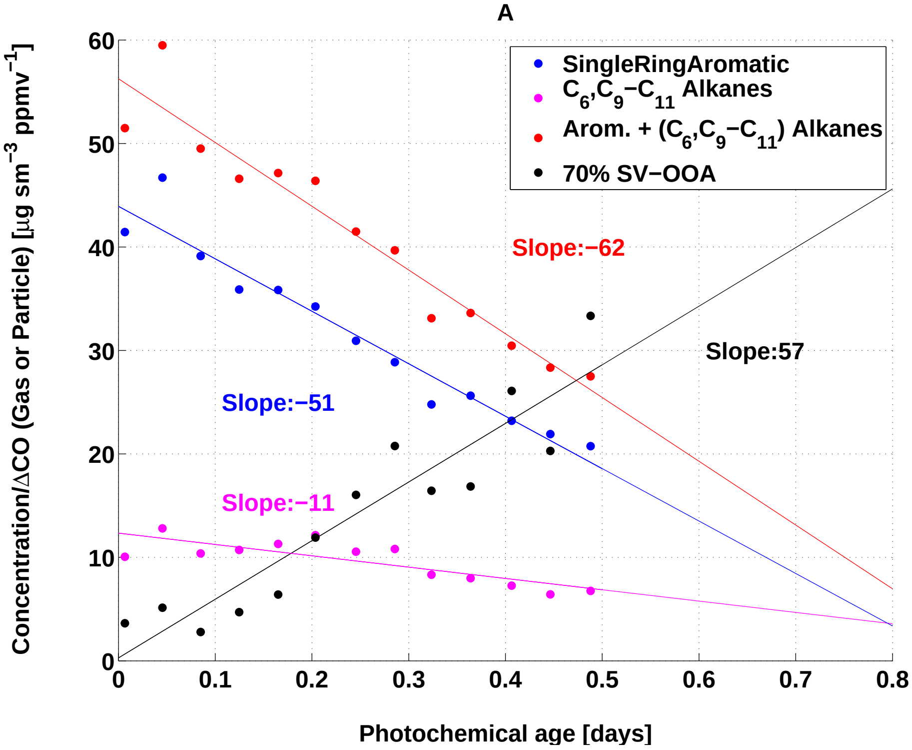

Fig. 4. Measured PMF OOA factor concentrations normalized by CO enhancement (ΔCO is the ambient CO minus the estimated background CO (105 ppb)) as functions of photochemical age. Also shown are lumped gas-phase VOC concentrations normalized by ΔCO. See Table 6 for the chemical speciation of each lumped species.